Journal of Soil Sciences and Agricultural Engineering

Journal homepage & Available online at: www.jssae.journals.ekb.eg

Drying Kinetics, Diffusivity, and Activation Energy for Hot Air Drying Of Different Shapes of Hayani Dates

Elfar, S. E.*; A. M. Matouk and Asmaa S. Elwasif

Faculty of Agriculture, Dep. of Agric. Eng., Mansoura University, Egypt.

Article Information
Received 22/ 9 /2025
Accepted 5/ 10/2025

ABSTRACT

One of the earliest techniques for preserving fruits is the drying process. Date palm fruit's with high fiber content, phenolic components, sugar, vitamins, and minerals make it a vital diet for human nutrition. The influence of shape (khalal halves, khalal pieces and rotab halves) and drying temperature ranged from 50 –70 °C on the drying kinetics of Hayani date palm fruits were studied. A constant air flow rate of 0.087 m^3s^{-1} was used. The activation energy (Ea) and effective moisture diffusivity (D_{eff}) were computed. Nine different thin-layer drying models were examined for describing the drying curves. The quality of date was assessed by estimating total and reducing soluble sugars content. The results showed that the drying process of dates took place during the falling rate period at all levels of air temperature. The average values of D_{eff} varied from 4.733 x 10^{-10} to 1.044 x 10^{-9} for khalal halves, 6.419 x10^{-10} to 9.5971 x 10^{-10} for khalal pieces and 7.3275 x 10^{-10} to 1.1607 x 10^{-9} m^2/s for rotab halves, respectively and Ea values were 35.1366, 15.6303 and 19.7316 kJ/mole for khalal halves, khalal pieces and rotab halves, respectively. The statistical analysis of fit tests revealed that Diamante *et al*. model proved a satisfactory fit for the experimental data for khalal halves while the mod. Henderson and Pabis model describe satisfactory data of khalal pieces and rotab halves. Total and reducing sugars increased with the increase of the drying air temperature for all date shapes.

Keywords: hot air – drying – date palm – thin layer -modeling.

INTRODUCTION

The date palm (Phoenix dactylifera L.) belongs to the Palmae family and is a monocotyledon. According to botany, date fruit is a berry with a single seed encased in a fleshy mesocarp, fibrous parchment-like endocarp, and fruit skin (pericarp). Depending on the kind and growth environment, date fruits can vary in size, shape, and weight. Dates are typically oblong, however certain types can become almost spherical. (Falade and Abbo, 2007).

Date palm fruit's having high fiber content, phenolic components, sugar, vitamins, and minerals make it a vital diet for human nutrition. (Ertekin and İpek 2020 and Amellal and Benamara, 2008).

In many nations, date palm fruit is a significant economic crop. In any date-packing or date-processing factory, drying air- cleaned, sorted, and water-washed dates is a crucial unit function. Later in the off-season, large amounts of extra dates are also dried and put to use. Bakery mixes and fillings can be flavored, sweetened, and adorned using dried dates. To be used as fruit pieces to add to morning cereals, some date cultivars need to be dried to a specific moisture content (Al-Awaadh *et al*., 2015).

The most significant ingredient in dates is carbohydrates, which make up around 78% of the fruit and give people rapid or easily accessible energy. The glucose and total sugar levels of date fruits can be greatly influenced by the variety and production locale. A great source of dietary fiber, dates can be contained anywhere from 6.4% to 11.5%, depending on the variety. There are both soluble and insoluble fibers in dates. The three main ingredients in dates are cellulose, hemicellulose, and lignin, which represent around 1.55%, 1.28%, and 2.01% of the total. Prior to the accumulation of sugar, the pectin level in dates reach its highest value, which is between 0.5% and 0.9%. This pectin is built during fruit growth. (Saikiran*et al*., 2018).

Al-Farsi *et al*., (2007) mentioned that, due to their numerous nutritional and functional benefits, unripened dates must be dried or dehydrated in order to create value-added products.

In humid environments, there is a possibility of fungal development, which lowers the dates' quality. Coliforms and fecal coliforms are the most common pathogens that attack dates. Unfavorable weather circumstances and a high risk of coliform assault cause dates to spoil to a very high degree (Al-Hooti *et al*., 2002). Drying and dehydration are necessary to stop these losses since they result in a decline in customer interest and export potential. (Falade and Abbo, 2007).

According to (Berhanu *et al*., 2017), palm fruit is a well-known fruit that has a high fiber, moisture, sugar, and polyphenol content. Because it contains phenolic compounds, it is a powerful antioxidant meal. Because of its sweet nature, it provides humans with energy when ingested. Vitamins A, C, and several B vitamins are also found in the palm. However, a high-water content results in a short shelf life as well as challenges with storage and transportation (Jia *et al*., 2019).

As the drying process reduces the moisture content, the fruit sugar (fructose) and minerals (phosphorous, copper, potassium, and iron) become more concentrated. In this case, drying is a crucial and required method to maximize the fruit's shelf life and use it efficiently from an economic standpoint. (Falade and Abbo, 2007; Jia *et al*., 2019; Li *et al*., 2019; Kayacan *et al*., 2020). Freeze drying (lyophilization), convective hot-air drying, microwave drying, solar drying, oven drying, spray drying, and vacuum drying are the most often used drying methods. (Ahmed *et al*., 2013; Alfaro *et al*., 2014).

* **Corresponding author.**
E-mail address: sea2082009@mans.edu.eg
DOI: 10.21608/jssae.2025.421753.1316

Elwakeel *et al*., (2023) revealed that, drying date fruits in Egypt is fraught with difficulties. Date fruits are gathered in great quantities each year. Only a tiny percentage of the yearly harvest is eaten locally fresh, but the farmers usually dry the fruits so they can sell them all year long, particularly during Ramadan.

Many foods may be shielded from deteriorating causes by the drying process, which is the oldest preservation technique. Drying is the process of eliminating water from solids in order to inhibit or stop the growth of germs or chemical processes. (Karaaslan, 2012). Vegetables and fruits are dried by solar drying in Mediterranean nations since it is an easy and inexpensive process, although it takes a long time to dry. In addition to the dried product's poor quality, it is extremely susceptible to microbial and enzymatic activity and is contaminated by dust and insects. (Andritsos *et al*., 2003). Hot air dryers (HAD) and sun dryers (SD) are examples of industrial dryers used to improve the quality of such dried products. (Ertekin and Yaldiz, 2004).

To guarantee safe storage, prevent marketing deterioration within a predetermined timeframe, facilitate processing, and allow product transportation, it is important to remove moisture from the product using heat. (Ambawat *et al*., 2022 and Eissa *et al*., 2024). The transmission of heat to the product and the following migration of moisture from the product to the surrounding medium are both intricate steps in the drying process. (Sahin and Dincer, 2005).

In addition to managing the drying process, mathematical modeling of drying is used to design and improve the existing drying systems or to construct new ones. Thin layer drying kinetics of agricultural products are described by a variety of mathematical models. These models fall into three categories: empirical, semi-empirical, and theoretical. (Demiray and Tulek, 2012).

Falade and Abbo (2007) examined the effects of variety and temperature within range of 50–80 ºC on the HAD pattern of date palm fruits. The findings showed that drying occurred throughout the period of falling rate. The impact of variety and rehydration temperatures between 15 and 45 ºC while maintaining the fruit-to-water ratio at 1:25 w/w were also examined. Using Fick's diffusion model, moisture transport during air drying and rehydration was explained, and Ea and D_{eff} were computed. The Arrhenius relation was used to illustrate the manner in which temperature affected the D_{eff} during air-drying and rehydration., which has Ea ranges of 35.17–44.02 $kJ.mol^{-1}$ and 30.29–40.29 $kJ.mol^{-1}$, respectively.

Convective hot air drying (CHAD) was investigated by Al-Awaadh *et al.* (2015) to dry date fruits at various air temperatures and velocities. Ten widely used models were examined to assess drying kinetics. Before and after drying, the fruit's color and texture were assessed. As drying temperature and air velocity dropped, drying time rose. The logarithmic, two-term exponential, and Henderson–Pabis models were the next best fits to the experimental data, after the Midilli and Kucuk model. Fruit texture and color were affected by drying. The drying temperature and air velocity should be between 60 and 70°C and 2 m/s, respectively, to reduce such variations.

Ertekin and İpek (2020) studied the effects of oven and Thermo-Gravimetric Analysis (TGA) drying on date palms using four temperature levels (50, 70, 90, and 110°C). The effect of the drying process on chemical changes in the structure of the dried date palms was evaluated using Fourier Transform Infrared (FTIR) analysis, and the fibrous structure of the palm fruit was visualized using Scanning Electron Microscopy (SEM). Microbiological analysis was also performed for fresh and dried dates to determine the effect of the drying process on the growth of microorganisms. The results showed that increasing the temperature decreased the drying time, while there was a negative effect on the color of the dried fruit, as the color turned darker with increasing temperature, and no significant change occurred in the chemical composition of the dried fruit. Furthermore, the drying time required by the TGA method was shorter than that of the oven method, and the microbiological load significantly decreased or disappeared with the drying process.

Matouk *et al.* (2010) used butane gas as a thermal energy source to evaluate a portable mechanical dryer for drying date palm fruits. The drying air temperature was set at (40, 50, 60, and 70 ºC), and its air velocity was set at 1, 1.5, and 2 m/s. They examined two empirical drying models (page and exponential) for describing the drying behavior of different conditions of dates (unpeeled, unpeeled treated and peeled treated). The total and reducing sugars of the dried date, the drying process's thermal efficiency, and the change in the date's moisture content during the drying process were also determined. The obtained results showed that both mathematical models were able to describe the drying kinetics of date fruits under the studied experimental conditions, while Page model was more accurate than the simple exponential model. The results also showed that with increasing the drying air temperature and velocity, the thermal efficiency of the dryer increased, from 32.23 to 69.84% for the unpeeled date, from 33.82 to 71.63% for the unpeeled treated date, and from 35.42 to 75.13% for the peeled date. Also, total and reducing sugars percentages decreased with the decrease of drying air temperature and air velocity. The unpeeled date had a reducing sugar range of 44.58 to 51.08% d.b., the unpeeled treated date had a range of 44.66 to 51.38% d.b., and the peeled date had a range of 44.58 to 51.76% d.b. However, for the same treatment, the total sugar levels varied from 56.01 to 64.73 % d.b., from 55.95 to 64.51 % d.b., and from 56.39 to 65.14 % d.b.

The current study uses a laboratory scale hot air drier to investigate the manner in which air temperature affects the drying behavior of three distinct date palm fruit forms. Nine mathematical models were tested, and the best one for explaining the drying characteristics under the conducted research conditions was chosen. The date palm fruit's activation energy and the impact of varying drying air temperature levels on the moisture diffusion rate were also determined. Lastly, the effect of different air temperature levels on the quality of the dried were determined in terms of both reduced and total sugars.

MATERIALS AND METHODS

Materials:

Hayani dates at the khalal and rotab stages of maturity (stages at which the fruit is fully ripe and readily edible) was harvested during the 2022 season, from a local date producing farm in Damietta governorate. The initial moisture content of the freshly harvested date was (212.923 ± 1% d.b.) for khalal stage and (194.859 ± 1% d.b.) for rotab stage. Until it was utilized for the experimental work, date samples were maintained in plastic bags in a freezer at -18°C. The date samples were removed from the freezer and allowed to come to room temperature within the lab prior to the experimental runs.

General description of the laboratory dryer:

The laboratory dryer developed and manufactured by Matouk *et al*., (2001) and located in the Food Processing Engineering Laboratory, Faculty of Agriculture, Mansoura University was used for the experimental work as shown in Fig. (1).

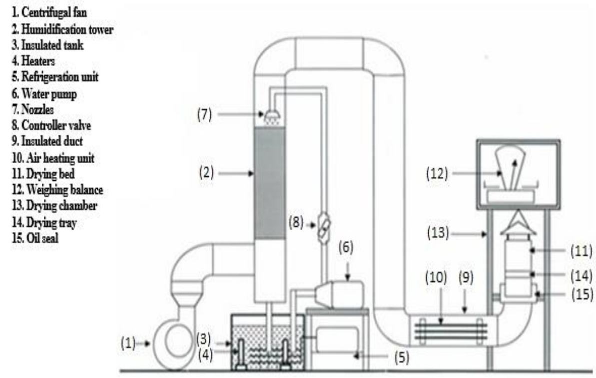

Fig. 1. Schematic diagram of the hot air drier.

The dryer contains the following:

A centrifugal blower:

Air is supplied to the dryer at room temperature by a 1.3 kW centrifugal blower with, after which it goes via a heating unit. The straight impeller of the blower can sustain a constant air flow rate during each experimental run.

The air heating unit:

Six electrical heaters, each with a 1 kW capacity, are part of the heating unit, which raises the air temperature to the necessary level for experimentation. The dry bulb temperature of the air was raised to the required level for each experimental run via a precise thermostat as it passed over a rank of insulated electrical heating elements fitted inside the section of air pipe. The heating elements were energized through a power regulator and sensor. The sensor was placed at the outlet of the pipe facing the air stream just below the drying tray. The action of the control may be described as: if the air temperature deviates from the pre-set value, the sensor sends a signal to the digital thermostat, which switches the heater on/off.

The air heating unit and the temperature controller adjusted the drying air temperature very satisfactorily. The temperature variation was very small (±0.1 ºC) from the set temperature.

The drying bed and chamber:

The hot air was passed from the heating unit to the drying bed via insulated steel pipe. The drying bed consisted of a galvanized steel cylinder (27 cm diameter and 70 cm long). It was suspended from the under hook of a balance standing in a rigid wood shelf above the chamber. The drying tray which contained the date sample was placed inside the steel cylinder. The drying chamber was made of wood (70×70×100 cm) with a roof on top, to constrain the air leaving the sample to flow down and leave the drying chamber through its base. It has also a hinged door which could be closed by latch to provide access to the inner cylinder to load or remove the sample. This ensured a minimal temperature gradient across the bed of date sample.

An oil seal was also placed at the base of the inner cylinder to ensure that all of the drying air passes through the drying bed (Fig. 2).

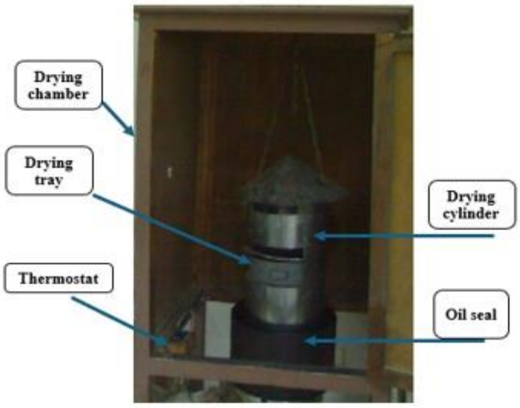

Fig. 2. Drying bed and chamber.

Measurements:

Moisture content: A hot air-drying oven set at 70 ºC for 16 hours, as advised by the AOAC (1990), was used to measure the moisture content of date fruit. Three replicates were used to test the moisture content of the date fruit. It should be noted that, unless otherwise noted, all moisture contents were represented on a dry basis.

Air temperature and speed: Throughout each experiment, a Trotec 2000S temperature and air speed meter was utilized to measure both variables. It contains a 12 mm diameter, 108 mm long measuring probe that is attached to the meter by a 1 m electrical connection. The temperature meter range is -20 to 70 ºC, with an accuracy of ± 0.1 ºC while the precision of the air speed meter is ± 0.01 m/s, and the measuring range is 0 to 20 m/s.

Weight of samples: A 200 ± 0.01 g capacity digital balance (AND EK-200GD) was used for measuring the date sample mass during the initial moisture content determination. Nevertheless, another digital balance (TR-6101) with (6000 ± 0.1 g) was used for follow up the changes in sample weight during drying experiments.

Thin layer drying experiments of date fruits:

The air temperature was maintained at around 50, 55, 60, 65, and 70 ºC while three distinct date shapes—rotab halves, khalal halves, and khalal pieces—were used for the experimental work. The air flow rate kept constant at 0.087 m^3/s. The drying apparatus was run for at least an hour using a dummy sample prior to the commencement of any experimental runs in order to stabilize the air flow rate and temperature. Once it was evident that the air flow rate and temperature had stabilized, a real date sample was spread over the drying tray, which was situated just inside the drying bed. Three samples, each weighing five grams, were collected simultaneously and stored in tins for moisture determination. After that, each tin was sealed with its lid and used to measure the initial moisture content.

The mass of the sample was measured at 5-minute intervals for the first hour then at 10-minute intervals for the second hour then at 20-min to the end of the experiment.

The experiments continued until the weight loss had nearly stopped, a sign that the date sample's moisture content had nearly reached equilibrium with the drying air. The final weight of the date samples was evaluated at the end of each drying test, and as previously mentioned, the date sample was then utilized to calculate the final moisture content.

Data processing and analysis:

The data of drying runs was recorded separately on paper sheets. Each sheet contained air temperature and balance reading which indicated weight loss of each run. The experimental sheets were processed before conducting any analysis. The action of the processing procedure was to convert the balance readings into moisture contents.

Calculation of moisture content at each data point:

The weight of the dry matter was assumed constant, and by knowing the initial moisture content of date fruit and the initial weight of sample and balance reading at different drying times, the calculations may be explained as follows:

$$WD = \frac{IWS}{1+IMC} \quad (1)$$

$$WWx = WSx - WD \quad (2)$$

$$MCx = \frac{WWx}{WD} \quad (3)$$

Where:

WD: weight of dry matter, g
IWS: Initial weight of sample, g
IMC: Initial moisture content, decimal
WW_x: Weight of water at time x, g
WS_x: Weight of sample at time x, g
MCx: Moisture content at time x, decimal

Evaluation of the drying data:

The following formulas were used to determine the moisture ratio (MR) and drying rate (DR):

$$MR = \frac{M_t - M_f}{M_o - M_f} \quad (4)$$

$$DR = \frac{M_i - M_t}{t - i} \quad (5)$$

Where:

M_o: initial moisture content, (%, dry basis); M_f: final moisture content, (%, dry basis); M_t: moisture content at any time t (%, dry basis); M_i: moisture content at time i (%, dry basis); t and i: start and end times, (min).

Thin layer drying models:

A non-linear regression analysis was achieved to fit the statistics into nine semi-theoretical thin layer models, frequently used to describe the drying curves of samples. The chosen models are Lewis's model, Henderson and Pabis's model, Page's model, Logarithmic model, two term exponential model, Modified Page's model, Modified Henderson and Pabis's model, the exponential linear combination (Elfar *et al* model), Diamante *et al.* model in the form of Eqs. (6) to (14), respectively as in Table (1).

Table 1. Selected mathematical models to demonstrate the drying process.

Model name	Model equation	Reference	
Lewis	$MR = exp(-k.t)$	(Lewis, 1921)	(6)
Henderson and Pabis	$MR = a\,exp(-k.t)$	(Henderson and Pabis, 1961)	(7)
Page	$MR = exp(-k\,t^n)$	(Page, 1949)	(8)
Logarithmic	$MR = a\,exp(-k\,t) + c$	(Wang *et al.*, 2007)	(9)
two terms	$MR = a\,exp(-k_0\,t) + b\,exp(-k_1\,t)$	(Henderson, 1974)	(10)
Modified Page	$\ln(-\ln MR) = \ln(k) + n\ln(t)$	(Yagcioglu, 1999)	(11)
Modified Henderson and Pabis (three terms)	$MR = a\,exp(-k_0 t) + b\,exp(-k_1\,t) + c\,exp(-k_2\,t)$	(Karathanos, 1999)	(12)
Elfar *et al* model	$MR = a + b\,exp(-k\,t) + c\,t$	(Elfar *et al.*, 2022)	(13)
Diamante *et al.* model	$\ln(-\ln MR) = a + b\ln(t) + c\,(\ln t)^2$	(Diamante *et al.*, 2010)	(14)

Where: MR is the moisture ratio (dimensionless); k, k_0, k_1 and k_2 are the drying constants (min^{-1}); a, b, c and n are the model constants (dimensionless); t is the drying time (min).

The most appropriate model was chosen as the best equation that could explain the drying kinetics with the highest coefficient of determination (R^2) and the lowest standard error (SE), reduced chi-square (χ^2), and root mean square error (RMSE) values (Pangavhane *et al.*, 1999; Sarsavadia *et al.*, 1999; Torki-Harchegani *et al.*, 2016).

$$R^2 = 1 - \frac{\sum_{i=1}^{N}(MR_{exp.,i} - MR_{calc.,i})^2}{[\sum_{i=1}^{N}(MR_{calc.,i} - MR)^2]} \quad (15)$$

$$\chi^2 = \frac{\sum_{i=1}^{N}(MR_{exp.,i} - MR_{calc.,i})^2}{N-n} \quad (16)$$

$$RMSE = \left[\frac{1}{N}\sum_{i=1}^{N}(MR_{calc.,i} - MR_{exp.,i})^2\right]^{1/2} \quad (17)$$

Where $MR_{exp;i}$ stands for the observed moisture ratio found in any measurement, $MR_{calc;i}$ is the calculated moisture ratio for this measurement and MR represent the average predicted value. N and n are the number of observations and constants, respectively (Pangavhane *et al.*, 1999; Sarsavadia *et al.*, 1999).

Effective moisture diffusivity and activation energy:

The effective moisture diffusivity (D_{eff}), which is determined by Fick's second law and is generally regarded as a crucial kinetics element, describes the movement of moisture from the substance to the environment during the falling rate stage. (Vega *et al.* 2007and Doymaz, 2007)

The D_{eff} for dates was calculated using the integrated equation of Fick's second law of diffusion for slab shape, as follows:

$$MR = \left(\frac{8}{\pi^2}\right) exp\left[\frac{-\pi^2\,D_{eff}\,t}{4L^2}\right] \quad (18)$$

Where, L is half thickness of date part; t is the drying time (sec) and D_{eff} is the effective moisture diffusivity (m^2s^{-1}).

When the ln of either side is taken, the equation corresponds to:

$$\ln(MR) = (-0.21) - \left[\frac{\pi^2}{4L^2}\,D_{eff}\,t\right] \quad (19)$$

D_{eff} are typically determined by plotting the experimental data in terms of ln(MR) versus time in Eq. (19), and the plot gives a straight line with a slope of

$$K_o = \frac{\pi^2\,D_{eff}}{4\,L^2} \quad (20)$$

The degree of moisture attachment to the wet substance determines the drying characteristics of wet products. Activation energy (Ea) is the relative ease with which water molecules pass through the samples after overcoming the energy barrier. The Arrhenius equation, which is shown below, expresses the effective diffusivity of a solid as a function of temperature. (Sanjuan *et al.*, 2003; Doymaz, 2007; Tunde Akintunde and Afon, 2010)

$$D_{eff} = D_o\,exp\left[\frac{-E_a}{R\,T}\right] \quad (21)$$

Where: D_o: pre-exponential factor of the Arrhenius equation (m^2s^{-1}); R: universal gas constant (8.314 $Jmol^{-1}\,K^{-1}$); E_a: activation energy ($kJ.mol^{-1}$); T: the absolute temperature (K).

By taking the natural logarithm of both sides, equation (21) becomes as follows

$$\ln(D_{eff}) = \ln(D_o) - \frac{E_a}{R\,T} \quad (22)$$

To get the values of the activation energy (Ea), the values of ln (D_{eff}) were plotted versus (1/T), and the slope of the fitted straight line is equal to (-Ea/R).

Assessment of the dried date fruits' quality:

The total and reduced sugar content of fresh and dried dates were compared in order to assess the impact of air temperature levels on the quality of the dried date fruits.

RESULTS AND DISCUSSION

Drying kinetics of date palm fruits:

Fig. (3) illustrates the impact of different levels of air temperatures on the drying rate and the corresponded moisture content of various date shapes.

As can be seen from Fig. (3), the drying process took place during the falling rate period, while the drying rate progressively dropped with the drying time for various date shapes. This demonstrated that the primary mechanism governing the flow of moisture through dates was diffusion, these findings agreed with those of Akpinar *et al.*, (2003) for pumpkin; Doymaz (2005) for okra; Elfar (2022) for tomato slices.

Additionally, it was observed that the rate of moisture removal was higher in the early phases of the drying process and subsequently reduced as the drying process progressed. This resulted from the dates' high initial MC, which raised the vapor pressure gradient and caused it to drop as the drying process goes towards the final moisture content. The effect of different studied shapes of date was reflected in varied moisture evaporation levels from the inner layers to the exterior depends upon the exposure area of each shape to the hot air. This condition causes different drying rates as reported by Wang *et al.* (2007). This was in line with the findings of Furthermore, the rate of drying and the increase in air temperature were directly correlated.

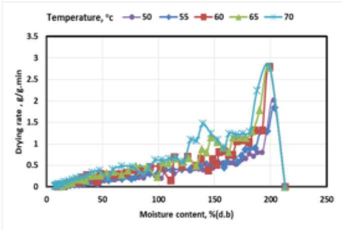

a) Khalal halves

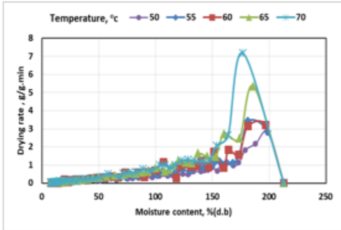

b) Khalal pieces

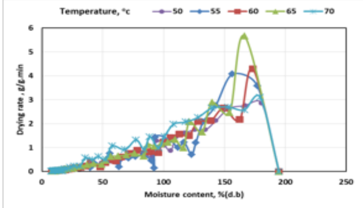

c) Rotab halves

Fig. 3. Relation between drying rate and moisture content for different shapes of dates at different air temperatures.

Fig. (4) Illustrates the change in date moisture content as related to drying time at different levels of drying air temperature for the three different studied date palm shapes. It can be noticed that air temperature had a great effect on the behavior of the drying process. It can be observed that with increasing the drying air temperature lower final moisture content can be achieved while the drying time is reduced.

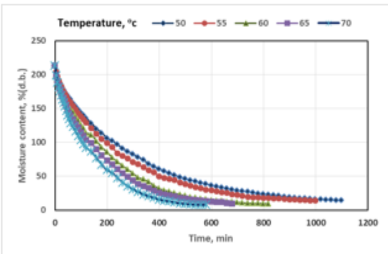

a) Khalal halves

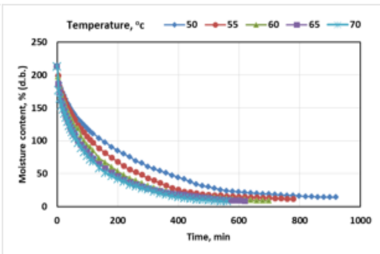

b) Khalal pieces

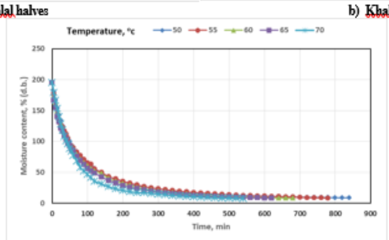

c) Rotab halves

Fig. 4. Relationship between drying time and the variation in date fruit moisture content at various drying air temperature.

As shown in Fig. (4), the final moisture content of dates decreased to 14.40 to 7.73 % (d.b.) for khalal halves, 13.90 to 7.65 % (d.b.) for khalal pieces and 8.99 to 7.73% (d.b.) for rotab halves at drying air temperature ranged from 50 to 70 ºc.

The impacts of date fruit shape on D_{eff} and Ea during the drying process:

For calculating (D_{eff}) of date palm fruits at different air-drying temperatures, ln (MR) was plotted against drying time and D_{eff} was extrapolated (Fig. 5). The plots satisfactorily described the drying behavior over the moisture ratio range ($0 \leq MR \leq 1.0$). Straight lines were obtained by linear regression with high determination coefficients (R^2 = 0.9341– 0.9771) for khalal halves, (R^2 = 0.9447– 0.9791) for khalal pieces and (R^2 = 0.9775 – 0.9859) for rotab halves. The relationship between ln (D_{eff}) and temperature (t) could be described by the following equation:

$$\ln(D_{eff}) = a - b\,(t) \qquad (23)$$

Tables (2) to (4) illustrate values of a, b and D_{eff} for different date shapes.

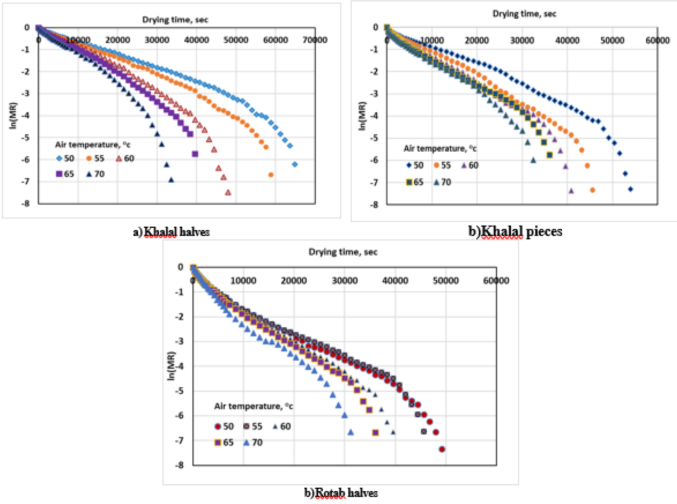

Fig. (5). Ln (MR) as related to drying time for different shapes of date at varying air temperature levels.

Table 2. Values of a, d and D_{eff} for khalal halves.

T, °c	a	b	R^2	D_{eff}, ($x10^{-10}$) m^2/s
50	0.138677	0.000073	0.9563	4.7337
55	0.153505	0.000086	0.9618	5.5767
60	0.270313	0.000120	0.9341	7.7814
65	0.094914	0.000119	0.9771	7.7166
70	0.229351	0.000161	0.9375	10.440

Table 3. Values of a, d and D_{eff} for khalal pieces.

T, °c	a	b	R^2	D_{eff}, ($x10^{-10}$) m^2/s
50	0.114647	0.000099	0.9447	6.4190
55	0.073848	0.000124	0.9686	8.0408
60	0.024210	0.000136	0.9609	8.8189
65	-0.162946	0.000129	0.9791	8.3650
70	-0.121548	0.000148	0.9764	9.5971

Table 4. Values of a, d and D_{eff} rotab halves.

T, °c	a	b	R^2	D_{eff}, ($x10^{-10}$) m^2/s
50	-0.318310	0.000120	0.9826	7.7181
55	-0.360541	0.000113	0.9775	7.3275
60	-0.266883	0.000140	0.9859	9.0783
65	-0.299031	0.000149	0.9842	9.6619
70	-0.278451	0.000179	0.9800	11.607

The results showed that D_{eff} varied from 4.733 x 10^{-10} to 1.044 x 10^{-9} m^2/s for khalal halves, 6.419 x10^{-10} to 9.5971 x 10^{-10} m^2/s for khalal pieces and 7.3275 x 10^{-10} to 1.1607 x 10^{-9} m^2/s for rotab halves, respectively. D_{eff} values mostly lie within the general range of 10^{-12}–10^{-8} m^2/s as reported for most food materials by Babalis and Belessiotis, (2004); Zogzas *et al*., (1996). Metwally *et al*., (2024) mentioned that D_{eff} for date palm fruit varied from 7.14 x 10^{-12} to 2.17 x 10^{-11} m^2/s. While Tireki (2023) found that D_{eff} for date palm fruit varied from 1.53 x 10^{-9} to 1.74 x 10^{-9} m^2/s.

The relationship between the reciprocal of air temperature (1/T) and the logarithm of effective moisture diffusivity ln (D_{eff}) is shown in Fig. (6). The results show that the value of activation energy (Ea) for mass diffusion were 35.1366 kJ/mole for khalal halves, 15.6303 kJ/mole for khalal pieces and 19.7316 kJ/mole for rotab halves, respectively. Generally, the values for Ea lie within the range of 12.7– 110 kJ/mol for most food materials (Zogzas *et al*., 1996). Differences in Ea for drying of dates could be due to the variation in geometry (surface area, shape factor) and composition of the studied fruit. Khalal halves had the highest activation energy of (35.1366 kJ/mol) followed by rotab halves (19.7316 kJ/mol) and khalal pieces which recorded the lowest activation energy of (15.6303 kJ/mole).

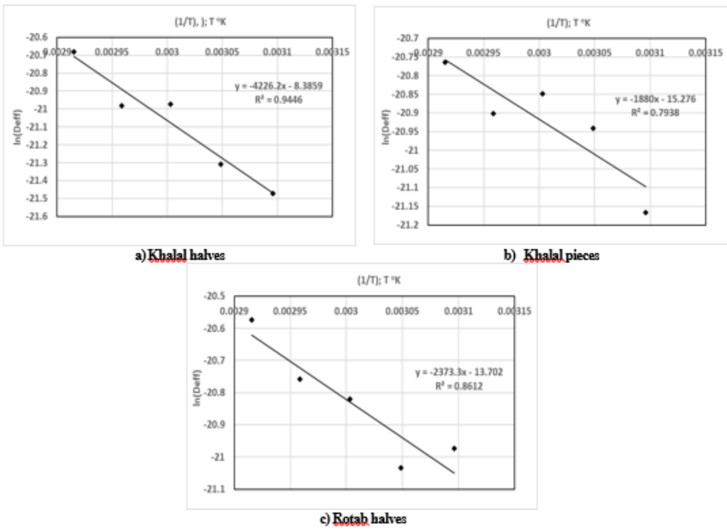

Fig. 6. Relationship between the reciprocal of air temperature (1/T) oK and the logarithm of effective moisture diffusivity ln (Deff)

Mathematical modeling:

The drying behavior was assesed and simulated using nine different thin layer drying models (Lewis model - Henderson and Pabis's model - Page model - Logarithmic model - two term model - modified Page model - Diamanate model - Elfar *et al*. model and modified Henderson and

Pabis's model). The examined models were compared to determine the best one in describing the drying kinetics of date fruits under the studied experimental conditions.

The results of the statistical computations are summarized in Tables (5 to 7).

Table 5. Statistical analysis of the examined models for khalal halves.

Model	T, °c	k						R^2	SE	X^2	RMSE
Lewis model	50	0.00417						0.9906	0.0264	0.0011	0.0325
	55	0.00491						0.9910	0.0267	0.0010	0.0317
	60	0.00666						0.9772	0.0441	0.0028	0.0526
	65	0.00693						0.9910	0.0282	0.0011	0.0322
	70	0.00905						0.9828	0.0366	0.0021	0.0448
Mean								0.9865	0.0324	0.0016	0.0388
		k	a								
Henderson and Pabis model	50	0.00436	1.14875					0.9861	0.0356	0.0064	0.0788
	55	0.00514	1.16591					0.9875	0.0357	0.0072	0.0833
	60	0.00717	1.31037					0.9673	0.0675	0.0193	0.1363
	65	0.00715	1.09956					0.9875	0.0351	0.0041	0.0626
	70	0.00969	1.25778					0.9736	0.0553	0.0138	0.1146
Mean								0.9804	0.0458	0.0102	0.0951
		k	n								
Page model	50	0.008383	0.87828					0.9940	0.0243	0.0007	0.0267
	55	0.008296	0.90391					0.9944	0.0235	0.0007	0.0256
	60	0.009879	0.91349					0.9877	0.0349	0.0015	0.0384
	65	0.012288	0.89069					0.9930	0.0263	0.0008	0.0279
	70	0.011723	0.93349					0.9914	0.0283	0.0010	0.0313
Mean								0.9921	0.0275	0.0010	0.0300
		k	a	c							
Logarithmic model	50	0.0033	0.9562	-0.0184				0.9988	0.0110	0.0001	0.0113
	55	0.0045	0.9590	-0.0174				0.9935	0.0181	0.0011	0.0323
	60	0.0046	0.9638	-0.0331				0.9978	0.0153	0.0002	0.0152
	65	0.0056	0.9509	-0.0190				0.9974	0.0163	0.0003	0.0160
	70	0.0067	0.9583	-0.0193				0.9971	0.0175	0.0003	0.0171
Mean								0.9969	0.0157	0.0004	0.0184
		a	k_o	b	k_1						
Two term model	50	0.4527	0.0035	0.4917	0.0035			0.9983	0.0117	0.0002	0.0130
	55	0.4557	0.0041	0.4925	0.0041			0.9983	0.0121	0.0002	0.0132
	60	0.4564	0.0050	0.4863	0.0050			0.9963	0.0174	0.0004	0.0192
	65	0.4427	0.0059	0.4966	0.0059			0.9969	0.0170	0.0003	0.0174
	70	0.4431	0.0071	0.5036	0.0071			0.9965	0.0183	0.0004	0.0185
Mean								0.9973	0.0153	0.0003	0.0163
		k	n								
Modified Page model	50	0.004321	0.8783					0.9971	0.0173	0.0006	0.0251
	55	0.004984	0.9039					0.9964	0.0190	0.0006	0.0238
	60	0.006380	0.9135					0.9911	0.0303	0.0011	0.0323
	65	0.007162	0.8907					0.9955	0.0221	0.0009	0.0292
	70	0.008841	0.9335					0.9908	0.0288	0.0011	0.0317
Mean								0.9942	0.0235	0.0009	0.0284
		a	b	c							
Diamante *et al.* model	50	-3.23742	0.18089	0.07140				0.9994	0.0092	0.0001	0.0107
	55	-3.44967	0.28902	0.06389				0.9993	0.0108	0.0002	0.0121
	60	-2.66784	-0.00656	0.09867				0.9987	0.0152	0.0003	0.0165
	65	-3.09255	0.25611	0.07019				0.9990	0.0142	0.0002	0.0146
	70	-3.01972	0.22303	0.08075				0.9981	0.0191	0.0004	0.0202
Mean								0.9989	0.0137	0.0002	0.0148
		a	b	k	c						
Elfar *et al.* model	50	0.1051	0.8404	0.0039	0.0001			0.9983	0.0097	0.0002	0.0130
	55	0.0744	0.8735	0.0044	0.00009487			0.9989	0.0107	0.0001	0.0106
	60	0.0661	0.9951	0.0044	0.000039365			0.9888	0.0181	0.0015	0.0367
	65	0.1101	0.8310	0.0066	0.0002			0.9977	0.0157	0.0003	0.0154
	70	0.1724	0.7825	0.0088	0.0004			0.9957	0.0167	0.0005	0.0215
Mean								0.9959	0.0142	0.0005	0.0194
		a	k_o	b	k_1	c	k_2				
The Modified Henderson and Pabis model (Three term)	50	0.2951	0.0035	0.3239	0.0035	0.3254	0.0035	0.9983	0.0117	0.0002	0.0130
	55	0.2927	0.0041	0.3251	0.0041	0.3260	0.0041	0.9983	0.0121	0.0002	0.0132
	60	0.3107	0.0048	0.3280	0.0048	0.3233	0.0048	0.9954	0.0161	0.0008	0.0268
	65	0.28337	0.0059	0.3265	0.0059	0.3294	0.0059	0.9969	0.0170	0.0003	0.0174
	70	0.2742	0.0071	0.3351	0.0071	0.3375	0.0071	0.9965	0.0183	0.0004	0.0185
Mean								0.9971	0.0150	0.0004	0.0178

Table 6. Statistical analysis of the examined models for khalal pieces.

Model	T, °c	k						R^2	SE	X^2	RMSE
Lewis model	50	0.005776						0.9922	0.03581	0.00234	0.04797
	55	0.007285						0.9947	0.03002	0.00177	0.04165
	60	0.008092						0.9972	0.02245	0.00161	0.03969
	65	0.008142						0.9940	0.03777	0.00639	0.07902
	70	0.009259						0.9942	0.03629	0.00607	0.07696
Mean								0.9945	0.03247	0.00364	0.05706
		k	a								
Henderson and Pabis model	50	0.005969	1.121478					0.9905	0.04265	0.00846	0.09043
	55	0.007434	1.076643					0.9940	0.03369	0.00485	0.06832
	60	0.008147	1.024505					0.9971	0.02315	0.00247	0.04869
	65	0.007722	0.849637					0.9932	0.03450	0.00123	0.03430
	70	0.008908	0.885549					0.9942	0.03310	0.00149	0.03759
Mean								0.9938	0.03342	0.00370	0.05587
		k	n								
Page model	50	0.015995	0.823284					0.9937	0.03222	0.00127	0.03502
	55	0.017244	0.847087					0.9950	0.02852	0.00098	0.03077
	60	0.01905	0.848138					0.9977	0.01882	0.00044	0.02055
	65	0.035359	0.746182					0.9985	0.01510	0.00028	0.01622
	70	0.041416	0.731218					0.9965	0.02306	0.00064	0.02472
Mean								0.9963	0.02354	0.00072	0.02546
		k	a	c							
Logarithmic model	50	0.0047	0.8903	-0.0056				0.9967	0.02497	0.00064	0.02465
	55	0.0062	0.8990	-0.0017				0.9974	0.02239	0.00052	0.02204
	60	0.0078	0.9040	0.0098				0.9979	0.02000	0.00041	0.01965
	65	0.0096	0.8489	0.0295				0.9954	0.02843	0.00084	0.02800
	70	0.0099	0.8343	0.0243				0.9950	0.02960	0.00092	0.02914
Mean								0.9965	0.02508	0.00067	0.02470
		a	k_o	b	k_1						
Two term model	50	0.1677	0.0765	0.8331	0.0044			0.9992	0.01090	0.00016	0.01238
	55	0.1547	0.1048	0.8491	0.0058			0.9995	0.00869	0.00011	0.00999
	60	0.1559	0.0844	0.8438	0.0069			0.9998	0.00598	0.00004	0.00602
	65	0.2545	0.0705	0.7357	0.0070			0.9998	0.00556	0.00003	0.00545
	70	0.2237	0.1597	0.7711	0.0079			0.9995	0.00913	0.00009	0.00894
Mean								0.9996	0.00805	0.00009	0.00856
		k	n								
Modified Page model	50	0.00658	0.823284					0.9947	0.03208	0.00247	0.04883
	55	0.00829	0.847087					0.9959	0.02799	0.00190	0.04278
	60	0.00937	0.848138					0.9975	0.02220	0.00178	0.04132
	65	0.01135	0.746182					0.9942	0.03604	0.00563	0.07328
	70	0.01285	0.731218					0.9941	0.03599	0.00591	0.07498
Mean								0.9953	0.03086	0.00354	0.05624
		a	b	c							
Diamante *et al.* model	50	-2.73893	0.1755104	0.068202				0.9974	0.01977	0.00047	0.02114
	55	-2.84901	0.271054	0.062280				0.9983	0.01603	0.00031	0.01696
	60	-3.07114	0.418026	0.0473414				0.9993	0.01030	0.00013	0.01122
	65	-2.57509	0.368186	0.042469				0.9995	0.00850	0.00009	0.00909
	70	-1.87332	0.074703	0.075079				0.9994	0.00898	0.00010	0.00941
Mean								0.9988	0.01271	0.00022	0.01356
		a	b	k	c						
Elfar *et al.* model	50	0.1920	0.7160	0.0066	-0.0002			0.9956	0.02195	0.00091	0.02905
	55	0.1250	0.7880	0.0077	-0.0002			0.9977	0.02121	0.00048	0.02112
	60	0.1369	0.7958	0.0098	-0.0002			0.9982	0.01662	0.00036	0.01814
	65	0.2140	0.7025	0.0145	-0.0004			0.9976	0.02051	0.00047	0.02056
	70	0.2200	0.6751	0.0153	-0.0004			0.9964	0.02219	0.00067	0.02460
Mean								0.9971	0.02050	0.00058	0.02269
		a	k_o	b	k_1	c	k_2				
The Modified Henderson and Pabis model (Three term)	50	0.1677	0.0765	0.4128	0.0044	0.4203	0.0044	0.9992	0.01090	0.00017	0.01238
	55	0.1547	0.1048	0.4211	0.0058	0.4280	0.0058	0.9995	0.00869	0.00011	0.00999
	60	0.1559	0.0844	0.4188	0.0069	0.4250	0.0069	0.9998	0.00598	0.00004	0.00602
	65	0.0629	0.4785	0.2232	0.0491	0.7138	0.0068	0.9999	0.00349	0.00001	0.00359
	70	0.1531	0.3591	0.1495	0.0324	0.6975	0.0073	0.9998	0.00535	0.00004	0.00577
Mean								0.9996	0.00688	0.00008	0.00755

Table 7. Statistical analysis of the examined models for rotab halves.

Model	T, °c	k						R^2	SE	X^2	RMSE
Lewis model	50	0.00780						0.9670	0.0575	0.0092	0.0950
	55	0.00753						0.9639	0.0612	0.0125	0.1107
	60	0.00904						0.9747	0.0510	0.0083	0.0899
	65	0.00969						0.9764	0.0491	0.0094	0.0957
	70	0.01157						0.9727	0.0489	0.0057	0.0748
Mean								0.9709	0.0535	0.0090	0.0932
		k	a								
Henderson and Pabis model	50	0.00721	0.72738					0.9551	0.0475	0.0040	0.0618
	55	0.00681	0.69730					0.9489	0.0488	0.0041	0.0629
	60	0.00842	0.76576					0.9654	0.0444	0.0028	0.0517
	65	0.00892	0.74154					0.9655	0.0423	0.0028	0.0514
	70	0.01073	0.75696					0.9587	0.0440	0.0048	0.0672
Mean								0.9587	0.0454	0.0037	0.0590
		k	n								
Page model	50	0.030507	0.78479					0.9979	0.0129	0.0002	0.0139
	55	0.041209	0.72659					0.9986	0.0102	0.0001	0.0106
	60	0.035176	0.77483					0.9991	0.0085	0.0001	0.0088
	65	0.044223	0.74300					0.9994	0.0058	0.0000	0.0064
	70	0.027103	0.85975					0.9958	0.0182	0.0004	0.0192
Mean								0.9982	0.0111	0.0002	0.0118
		k	a	c							
Logarithmic model	50	0.0123	0.9089	0.0258				0.9926	0.0241	0.0006	0.0238
	55	0.0118	0.8621	0.0315				0.9887	0.0289	0.0009	0.0286
	60	0.0131	0.8929	0.028				0.9921	0.0250	0.0006	0.0246
	65	0.0136	0.8687	0.0266				0.9917	0.0251	0.0007	0.0247
	70	0.0169	0.9654	0.0218				0.9984	0.0122	0.0002	0.0119
Mean								0.9927	0.0230	0.0006	0.0227
		a	k_o	b	k_1						
Two term model	50	0.4870	0.0288	0.5134	0.0064			0.9999	0.0030	0.00001	0.0029
	55	0.3863	0.0423	0.5995	0.0068			0.9983	0.0110	0.00013	0.0110
	60	0.4247	0.0349	0.5644	0.0074			0.9998	0.0044	0.00002	0.0043
	65	0.3073	0.0577	0.6724	0.0090			0.9990	0.0083	0.00008	0.0083
	70	0.7899	0.0211	0.2141	0.0065			0.9997	0.0054	0.00003	0.0053
Mean								0.9993	0.0064	0.0001	0.0063
		k	n								
Modified Page model	50	0.011717	0.78479					0.9830	0.0421	0.0048	0.0680
	55	0.012412	0.72659					0.9804	0.0458	0.0068	0.0811
	60	0.013295	0.77483					0.9852	0.0395	0.0048	0.0680
	65	0.015038	0.74300					0.9868	0.0372	0.0054	0.0717
	70	0.015042	0.85975					0.9868	0.0357	0.0029	0.0521
Mean								0.9844	0.0401	0.0049	0.0682
		a	b	c							
Diamante *et al.* model	50	-3.92470	0.98928	-0.02185				0.9994	0.0081	0.00009	0.0091
	55	-3.31055	0.78434	-0.00624				0.9991	0.0099	0.00011	0.0103
	60	-3.29883	0.75124	0.00261				0.9960	0.0155	0.00088	0.0287
	65	-2.73425	0.55364	0.02127				0.9998	0.0050	0.00003	0.0050
	70	-4.35089	1.23401	-0.04308				0.9995	0.0080	0.00007	0.0078
Mean								0.9988	0.0093	0.0002	0.0122
		a	b	k	c						
Elfar *et al.* model	50	0.1205	0.8442	0.0155	-0.0002			0.9955	0.01574	0.00043	0.02005
	55	0.1444	0.7841	0.0158	-0.0002			0.9942	0.01985	0.00043	0.02000
	60	0.14285	0.8104	0.0171	-0.0002			0.9941	0.01511	0.00046	0.02049
	65	0.1362	0.78752	0.01755	-0.0003			0.9936	0.01928	0.00060	0.02335
	70	0.0832	0.9169	0.0189	-0.0002			0.9989	0.00644	0.00012	0.01034
Mean								0.9953	0.0153	0.0004	0.0188
		a	k_o	b	k_1	c	k_2				
The Modified Henderson and Pabis model (Three term)	50	0.2753	0.0388	0.3180	0.0161	0.4106	0.0058	0.9999	0.0025	0.00001	0.0025
	55	0.1828	0.1083	0.4605	0.0164	0.3634	0.0052	0.9992	0.0079	0.00007	0.0078
	60	0.0270	9.2399	0.4313	0.0317	0.5417	0.0072	0.9998	0.0035	0.00001	0.0034
	65	0.1311	0.2031	0.4040	0.0227	0.4638	0.0073	0.9998	0.0035	0.00001	0.0035
	70	0.3970	0.0211	0.3929	0.0211	0.2141	0.0065	0.9997	0.0054	0.00003	0.0053
Mean								0.9997	0.0045	0.00003	0.0045

At all air temperature levels, the data demonstrated a good agreement between the experimental data and the values calculated using the examined mathematical models and this is confirmed by the high values of R^2 which ranged from (0.9804 to 0.9989) for khalal halves , (0.9938 to 0.9996) for khalal pieces and (0.9587 to 0.9997) for rotab halves and the low values of (SE), (χ^2) and (RMSE). It could be noted from table (4) that for khalal halves, Diamanate model gave the highest value of (R^2 = 0.9989) the lowest values for (SE = 0.0137), (χ^2 = 0.0002) and (RMSE = 0.0148). Also, table (4) shows that Henderson and Pabis model gave the lowest average values of (R^2 = 0.9804) and the highest average values of (SE = 0.0458), (χ^2 = 0.0102) and (RMSE = 0.0951). Therefore, it was logical to believe that the Diamanate *et al.* model properly depicted the drying behavior of khalal halves date palm in the tested hot air drier followed by two term model. Also, it also could be noted from table (5) that for khalal pieces, the modified Henderson and Pasis model gave the highest value of (R^2 = 0.9996) the lowest values for (SE = 0.0688), (χ^2 = 0.00008) and (RMSE = 0.00755). As shown in the Table that Henderson and Pabis model gave the lowest average values of (R^2 = 0.9938) and the highest average values of (SE = 0.03342), (χ^2 = 0.0037) and (RMSE = 0.05587). Therefore, it was logical to believe that the modified Henderson and Pasis model depicted the drying behavior of khalal pieces date palm in a hot air drier followed by the two-term model.

It could be also noted from table (6) that for rotab halves, the modified Henderson and Pasis model gave the highest value of (R^2 = 0.9997) the lowest values for (SE = 0.0045), (χ^2 = 0.00003) and (RMSE = 0.0045). Meanwhile Henderson and Pabis model gave the lowest average values of (R^2 = 0.9587) and the highest average values of (SE = 0.0454), (χ^2 = 0.0037) and (RMSE = 0.0590). Therefore, it was logical to believe that the modified Henderson and Pasis model depicted the drying behavior of rotab halves followed by the two-term model. The experimental and calculated moisture ratios of the chosen models are displayed in Fig. (7).

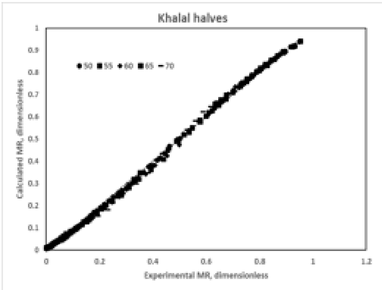

a) Diamanate *et al.* model

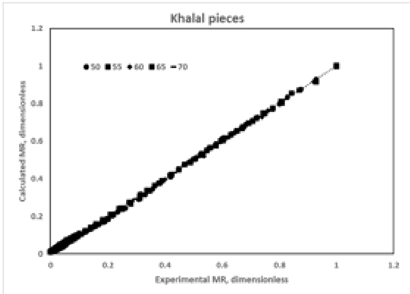

b) Modified Henderson and Pasis model

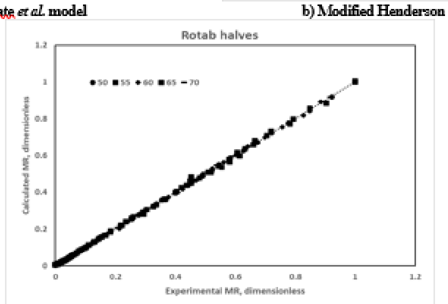

C) Modified Henderson and Pasis model

Fig. 7.Comparison between MRcalc and MRexp for the selected models.

Effect of drying temperature on total sugar (TS) and reducing sugars (RS) of the dried dates:

The results presented in Table (8) showed that TS and RS increased with the increase of the drying air temperature for all studied date shapes. It can be seen that, at the minimum drying air temperature of 50 ^{0}C, the average values of TS for khalal halves, khalal pieces and rotab halves were 51.26,57.04 and 69.46 % (d.b) while the average values of RS were 21.049, 21.753 and 21.753 % (d.b) respectively. At the maximum drying air temperature of 70 ^{0}C, the average value of TS was 64.67, 72.67 and 92.10 % (d.b) and the average RS were 22.054, 23.259 and 23.961 % (d.b), respectively. This observation may be attributed to long time of fruits exposure to heat which led to decrease the RS during the drying process and the browning reaction. These results are consistent with the results obtained by Ibrahim *et al*., (2008) and EL-Ghazali and Hussin (1999). These results also agreed with those of Nezam El–Din (1997), who found that the TS and RS in (Amhat variety) were increased by increasing the temperature from 40°C to 70°C while it decreased at 80°C.

Table 8. Total and reducing soluble sugars % (d.b) of the dried date.

Air Temp.,	Total soluble sugars, % (d.b)			Reducing sugar, %(d.b)		
ºC	Khalal halves	Khalal pieces	Rotab halves	Khalal halves	Khalal pieces	Rotab halves
50	51.26	57.04	69.46	21.049	21.753	21.753
55	59.95	62.32	81.32	21.250	22.555	23.058
60	61.80	65.47	85.12	21.753	22.556	23.158
65	63.88	65.80	91.92	21.953	23.058	23.559
70	64.67	72.67	92.10	22.054	23.259	23.961

CONCLUSION

Drying characteristics of three different shapes of Hayani date palm fruits were studied using heated air dryer (HAD) at air temperature ranging from 50 to 70 ºC and constant air flow rate of 0.087 m^3/s. The date was dried at all temperature levels throughout the falling drying rate period, however the constant drying rate period was not observed. Nine different thin-layer drying models were tested for describing the drying curves. The statistical analysis of fit tests revealed that Diamante *et al.* model provided a satisfactory fit for the experimental data for khalal halves while the modified Henderson and Pabis model satisfactory described the data of khalal pieces and rotab halves. The average values of effective moisture diffusivity varied from 4.733 x 10^{-10} to 1.044 x 10^{-9} for khalal halves, 6.419 x10^{-10} to 9.5971 x 10^{-10} for khalal pieces and 7.3275 x 10^{-10} to 1.1607 x 10^{-9} m^2/s for rotab halves, respectively and the activation energy were 35.1366 for khalal halves, 15.6303 for khalal pieces and 19.7316 kJ/mole for rotab halves, respectively. The total and reducing sugars increased with the increase of drying air temperature for all studied date shapes.

REFERENCES

Ahmed, N., J. Singh, H. Chauhan, P.G.A. Anjum, and H. Kour. (2013). Different drying methods: Their applications and recent advances. Int. J. Food Nutri. Saf. 4(1):34–42

Akpinar E.K.; Bicer Y., and Yildiz C. (2003) Thin layer drying of red pepper. J Food Eng 59:99–104

Al-Awaadh, A. M., Hassan, B. H., & Ahmed, K. M. (2015). Hot air-drying characteristics of Sukkari date (Phoenix dactylifera L.) and effects of drying condition on fruit color and texture. *International Journal of Food Engineering*, *11*(3), 421-434.

Alfaro, S., A. Mutis, A. Quiroz, I. Seguel, and E. Scheuermann. (2014). Effects of drying techniques on murtilla fruit polyphenols and antioxidant activity. J. Food Res. 3(5)

Al-Farsi, M., Alasalvar, C., Al-Abid, M., Al-Shoaily, K., Al-Amry, M., & Al-Rawahy, F. (2007). Compositional and functional characteristics of dates, syrups, and their by-products. *Food chemistry*, *104*(3), 943-947.

Al-Hooti, S. N., Sidhu, J. S., Al-Saqer, J. M., and Al-Othman, A. (2002). Chemical composition and quality of date syrup as affected by pectinase/cellulase enzyme treatment. *Food chemistry*, *79*(2), 215-220.

Ambawat, S., Sharma, A., and Saini, R. K. (2022). Mathematical modeling of thin layer drying kinetics and moisture diffusivity study of pretreated Moringa oleifera leaves using fluidized bed dryer. *Processes*, *10*(11), 2464.

Amellal, H., & Benamara, S. (2008). Vacuum drying of common date pulp cubes. *Drying Technology*, *26*(3), 378-382.

Andritsos, N., Dalampakis, P., and Kolios, N. (2003). Use of geothermal energy for tomato energy. GMC Bulletin (March), 9–13.

AOAC (1990) Official method of analysis. Association of Official Analytical Chemists (No. 934.06), Arlington

Babalis, S. J., and Belessiotis, V. G. (2004). Influence of the drying conditions on the drying constants and moisture diffusivity during the thin-layer drying of figs. *Journal of food Engineering*, *65*(3), 449-458.

Berhanu, D., M. Safdar, and F. Eihab. (2017). Market acceptability of dried dates at the unripe "Bisr" stage in United Arab Emirates. Emir. J. Food Agric. 29(9):674–684.

Demiray, E., and Tulek, Y. (2012). Thin layer drying of tomato (Lycopersicon esculentum Mill. cv. Rio Grande) slices in a convective hot air dryer. Heat and Mass Transfer, 48(5), 841-847.

Diamante L. M.; Ihns R.; Savage G. P., and Vanhanen L. (2010). A new mathematical model for thin layer drying of fruits. International journal of food science & technology, 45(9), 1956-1962.

Doymaz I. (2005). Drying characteristics and kinetics of okra. Journal of Food Engineering, 69, 275–279.

Doymaz I. (2007) Air-drying characteristics of tomatoes. J. Food Eng. 78:1291–1297

Eissa, A. S., Gameh, M. A., Mostafa, M. B. & Elwakeel, A. E. (2024). Some engineering factors affecting utilization of solar energy in drying tomato fruits introduction. *Aswan Univ. J. Environ. Stud.* **5**, 52–68

EL Ghazali M.N. and F. Hussin (1999). Effect of sun drying and mechanical drying on composition and libid, phospholipids fractions of Aswan dry dates. Egypt J. Hort. 2,(2) 209-215

Elfar, S. E. (2022). Thin Layer Drying Characteristics of Tomato Slices in A Hot Air Dryer. *Journal of Soil Sciences and Agricultural Engineering*, *13*(12), 421-428.

Elwakeel, A. E., Wapet, D. E. M., Mahmoud, W. A. E. M., Abdallah, S. E., Mahmoud, M. M., Ardjoun, S. A. E. M., and Tantawy, A. A. (2023). Design and implementation of a pv-integrated solar dryer based on internet of things and date fruit quality monitoring and control. *International Journal of Energy Research*, *2023*(1), 7425045.

Ertekin, C., and Yaldiz, O. (2004). Drying of eggplant and selection of a suitable thin layer drying model. Journal of Food Engineering, 63, 349–359.

Ertekin, Ö., and İpek, Y. (2020). Modeling of drying processes of dates (Phoenix, Arecaceae) with oven or TGA and microbiological properties of fresh and dried dates. *International Journal of Fruit Science*, *20*(sup3), S1530-S1538.

Falade, K. O., and Abbo, E. S. (2007). Air-drying and rehydration characteristics of date palm (Phoenix dactylifera L.) fruits. *Journal of Food Engineering*, *79*(2), 724-730.

Henderson S.M., and Pabis S., (1961). Grain drying theory. II. Temperature effects on drying coefficients. J. Agric. Eng. Res., 6, 169–174

Henderson, S. M. (1974). Progress in developing the thin layer drying equation. Transactions of the ASAE, 17(6), 1167-1168.

Ibrahim, A. A., Abd El Fadeel, M. G., Ghoneim, S. I., and Abd El Razicl, F. A. (2008). Effect of drying methods on chemical composition and sensory properties of Amry date. *Journal of Food and Dairy Sciences*, *33*(1), 353-361.

Jia, Y., I. Khalifa, L. Hu, W. Zhu, J. Li, K. Li, and C. Li. (2019). Influence of three different drying techniques on persimmon chips characteristics: A comparison study among hot-air, combined hot-air-microwave, and vacuum-freeze drying techniques. Food Bioprod. Process. 118:67–76. doi: 10.1016/j.fbp.2019.08.018.

Karaaslan, S. 2012. Meyve ve sebzelerin mikrodalga destekli kurutma sistemleri ile kurutulması. Süleyman Demirel Üniversitesi Ziraat Fakültesi Dergisi 7(2):123–129.

Karathanos, V.T. (1999). Determination of water content of dried fruits by drying kinetics. J. Food Eng. 39, 337–344.

Kayacan, S., S. Karasua, P.K. Akman, H. Goktas, I. Doymaz, and O. Sagdic. (2020). Effect of different drying methods on total bioactive compounds, phenolic profile, in vitro bioaccessibility of phenolic and HMF formation of persimmon. LWT - Food Sci. Techn. 118:108830. doi: 10.1016/j.lwt.2019.108830.

Lewis W. K. (1921). The rate of drying of solid materials. Industrial and Engineering Chemistry, 13(5), 427-432.

Li, D., H. Xie, Z. Liu, A. Li, J. Li, B. Liu, X. Liu, and D. Zhou. (2019). Shelf-life prediction and changes in lipid profiles of dried shrimp (Penaeusvannamei) during accelerated storage. Food Chem. Volume 297, 1 November. 2019:124951. doi: 10.1016/j.foodchem.2019.124951.

Matouk, A. M.; Abd El-Latif, S. M.; El-Hadidi, Y. M., and Tharwat, A. (2001). Drying of ear corn: Part I: Determination of drying parameters. Misr J. Agric. Engng, 18(3), 805-820.

Matouk, A.M.; M.M. El-Kholy; M.A. El-Sadany; and A.E. Abd El-Aziz (2010). Thin Layer Drying of Hayani Date Using A Portable Dryer. *J. of Soil Sciences and Agricultural Engineering, Vol.1 (4):323-337*

Metwally, K. A., Oraiath, A. A. T., Elzein, I. M., El-Messery, T. M., Nyambe, C., Mahmoud, M. M., ... & Elwakeel, A. E. (2024). The mathematical modeling, diffusivity, energy, and enviro-economic analysis (MD3E) of an automatic solar dryer for drying date fruits. Sustainability, 16(8), 3506

Mittal, G. S. (1999). Mass diffusivity of food products. Food Research International, 15, 19–66

Nezam El-Din, M. A. and Abd El-Hameed, A.K. (1997) Chemical and technological study on Egyptian Amhat date.2-Drying of Egyptian Amhat date. Egypt J. Agric. Res., 75 (4): 1154 – 1160.

Page, G. E. (1949). Factors Influencing the Maximum Rates of Air-Drying Shelled Corn in Thin layers. Purdue University.

Pangavhane, D. R., R. L. Sawhney, and P. N. Sarsavadia, (1999). Effect of various dipping pre-treatment on drying kinetics of Thompson seedless grapes. Journal of Food Engineering, 39, 211–216

Ramesh, M. N., Wolf, W., Tevini, D., and Jung, G. (2001). Influence of processing parameters on the drying of spice paprika. *Journal of Food Engineering*, *49*(1), 63-72.

Sahin A.Z., and Dincer I. (2005) Prediction of drying times for irregular shaped multi-dimensional objects. J Food Eng 71(1):119–126

Saikiran, K. C. S., Reddy, N. S., Mn, L., and Venkatachalapathy, N. (2018). Different drying methods for preservation of dates: a review. *Curr J Appl Sci Technol*, *29*, 1-10.

Sanjuan, N., Lozano, M., Garcia-Pascal, P., and Mulet, A. (2003). Dehydration kinetics of red pepper (Capsicum annuum L var Jaranda). Journal of the Science of Food and Agriculture, 83, 697–701.

Sarsavadia, P. N., R. L. Sawhney, D. R. Pangavhane, and S. P. Singh, (1999). Drying behaviour of brined onion slices. Journal of Food Engineering, 40, 219–226

Tireki, S. Effective diffusivity determination of date (Phoenix dactylifera L.) leather in infrared drying: Effect of cooking time. Ni˘gde Ömer Halisdemir Üniversitesi Mühendislik Bilim. Derg. 2023, 12, 1558–1565.

Torki-Harchegani M., M. Ghasemi-Varnamkhasti, D. Ghanbarian, M. Sadeghi, M. Tohidi, Dehydration characteristics and mathematical modelling of lemon slices drying undergoing oven treatment, Heat Mass Transf. Und Stoffuebertragung. 52 (2016) 281–289

Tunde-Akintunde T.Y., and Afon A.A. (2010) Modelling of hot-air drying of pretreated cassava chips. Agric Eng. Int: CIGR Journal 12(2):34–41

Vega A.; Fito P.; Andrés A., and Lemus R. (2007) Mathematical modeling of hot-air drying kinetics of red bell pepper (var. Lamuyo). J Food Eng 79:1460–1466

Wang Z.; Sun J.; Liao X.; Chen F.; Zhao G.; Wu J., and Hu X. (2007) Mathematical modeling on hot air drying of thin layer apple pomace. Food Res Int 40:39–46

Yagcioglu A., (1999). Drying Techniques of Agricultural Products, Ege Univ. Fac. Agric. Publ.

Zogzas N. P.; Maroulis Z. B., and Marinos-Kouris, D. (1996). Moisture diffusivity data compilation in foodstuffs. Drying Technology, 14, 2225–2253

حركية التجفيف والانتشارية وطاقة التنشيط لتجفيف أشكال مختلفة من البلح الحياني بالهواء الساخن

سامي ابراهيم الفار ، أحمد محمود معتوق و أسماء سمير الوصيف

كلية الزراعة – قسم الهندسة الزراعية – جامعة المنصورة – مصر.

الملخص

تمثل طريقة التجفيف واحدة من أقدم طرق الحفظ المستخدمة لحفظ الفاكهة. تعتبر ثمار البلح غذاء مهم في تغذية الإنسان لاحتوائها على بعض الفيتامينات والمعادن والسكر والمكونات الفينولية والألياف. تمت دراسة تأثير ثلاثة أشكال مختلفة (أنصاف الخلال وقطع الخلال وأنصاف الرطب) وخمسة مستويات مختلفة لدرجة حرارة التجفيف في مدى ٥٠-٧٠ °م على سلوك التجفيف بالهواء الساخن عند معدل تدفق هواء تجفيف ثابت قدره ٠,٠٨٧ م ٣ / ثانية. تم حساب كل من انتشار الرطوبة الفعال وطاقة التنشيط كما تم اختبار تسعة نماذج مختلفة لتجفيف الطبقة الرقيقة لوصف منحنيات التجفيف. تم أيضا تقييم جودة التمور من خلال تقدير محتوى السكريات الذائبة الكلية والمختزلة. أظهرت النتائج أن عملية تجفيف التمور حدثت خلال فترة معدل التجفيف المتناقص في جميع مستويات درجة حرارة الهواء وتراوحت القيم المتوسطة لانتشار الرطوبة الفعال بين ٤,٧٣٣ × ١٠-١٠ و١,٠٤٤ × ١٠-٩ لأنصاف الخلال، و٦,٤١٩ × ١٠-١٠ إلى ٩,٥٩٧١ × ١٠-١٠ لقطع الخلال، و٧,٣٢٧٥ × ١٠-١٠ إلى ١,١٦٠٧ × ١٠-٩ م٢/ثانية لأنصاف الرطب، على التوالي. وكانت طاقة التنشيط ٣٥,١٣٦٦ لأنصاف الخلال، و١٥,٦٣٠٣ لقطع الخلال، و١٩,٧٣١٦ كيلوجول/مول لأنصاف الرطب، على التوالي. وكشف التحليل الإحصائي أن نموذج Diamanate *et al* أكثر ملاءمة لوصف البيانات التجريبية لأنصاف الخلال، بينما وصف نموذج Mod. Henderson and Pabis البيانات التجريبية لقطع الخلال وأنصاف الرطب بصورة مرضية. ارتفعت نسبة السكريات الكلية والمختزلة مع زيادة درجة حرارة هواء التجفيف لجميع أشكال التمور.

الكلمات الدالة: الهواء الساخن – التجفيف – البلح – طبقة رقيقة – النمذجة.